Atmospheric Research, 31 (1994) 235–252
Elsevier Science B.V., Amsterdam

New microphysics sensor for aircraft use

H. Gerber[a], B.G. Arends[b] and A.S. Ackerman[c]
[a]*Gerber Scientific Inc., 1643 Bentana Way, Reston, VA 22090, USA*
[b]*Netherlands Energy Research Foundation (ECN), P.O. Box 1, 1755 ZG Petten, Netherlands*
[c]*Department of Atmospheric Sciences, AK-40, University of Washington, Seattle, WA 98195, USA*

(Received March 16, 1993; revised and accepted August 28, 1993)

ABSTRACT

A new optical sensor, PVM-100A, for aircraft cloud-microphysical measurements is described. The sensor measures the liquid water content (LWC), the integrated particle surface area (PSA) and the effective droplet radius r_e of cloud droplets. The measurements are simultaneous, are made on a cloud volume of 1.25 cm^3, are made in situ and in real time, and have a maximum bandwidth of 5 KHz.

Results are presented of calibrations of the PVM-100A in the fog-wind tunnel at ECN, Petten, The Netherlands where the LWC channel was compared to gravimetric measurements of droplets collected in filters, and the PSA channel was compared to measurements made with a corrected FSSP-100.

The PVM-100A, CSIRO (King) and Johnson-Williams hot-wire probes, and another FSSP-100 were compared on flights made with the University of Washington C-131A aircraft in stratocumulus clouds during the 1992 ASTEX experiment near the Azores. The hot-wire probes were unable to resolve fine features in broken clouds, because of insufficient time response; the uncorrected FSSP-100 underestimated LWC when either LWC or droplet sizes was large and the measurements of r_e made with the FSSP-100 and PVM-100A showed a large systematic difference. A simple method is proposed for retrieving accurate FSSP-100 droplet spectra using this difference and PVM-100A measurements of LWC.

RÉSUMÉ

On décrit un nouveau détecteur optique, le PVM-lOOA, pour les mesures microphysiques par avion dans les nuages. L'instrument mesure le contenu en eau liquide (LWC), la surface totale des particules (PSA), et le rayon effectif r_e des gouttelettes de nuage. Les mesures sont réalisées simultanément et en temps réel sur un volume nuageux de 1,25 cm^3, et elles ont une largeur de bande maximale de 5 KHz.

On présente les résultats des calibrations du PVM-lOOA dans le tunnel à vent et brouillard de ECM, Petten (Pays-Bas). Le canal LWC est calibré par pesée de gouttelettes captées sur filtres, et le canal PSA est testé par comparaison avec un FSSP-100 corrigé.

A l'occasion de l'experience ASTEX 1992 aux Açores, on a procédé à des comparaisons dans des stratocumulus, à bord du C-131A de l'Université de Washington, du PVM-100A, des sondes à fil chaud du CSIRO (King) et du Johnson-Williams, ainsi que d'un autre FSSP-100. Les sondes à fil chaud ne sont pas adaptées à la mesure des structures fines dans des nuages fragmentés à cause de leur temps de réponse insuffisant. Le FSSP-100 non corrigé sous-estime LWC lorsque LWC est élevé ou lorsque les gouttes sont grosses. Enfin les mesures de r_e avec le FSSP-100 et le PVM-100A présentent une différence systématique importante. On propose une méthode simple pour restituer des spectres de gouttelettes précis à l'aide du FSSP-100 en utilisant cette différence et les mesures de LWC au PVM-100A.

SSDI 0169-8095(93)E0045-Z

INTRODUCTION

We describe the principle of operation, the configuration and the testing of a new microphysics sensor, PVM-100A, designed for aircraft use (Gerber, 1992). This two-channel sensor measures optically and in situ the liquid water content (LWC) and the total particle surface area (PSA) of cloud droplets, using a technique similar to the one described by Wertheimer and Wilcock (1976). This sensor also provides the effective droplet radius, r_e, because $r_e \propto \mathrm{LWC/PSA}$. The value of r_e in clouds is useful in parameterizing the radiative effect of clouds (Hansen and Travis, 1974); and the reduction of r_e in clouds due to anthropogenic influences may counter in part global warming due to the increase in CO_2 (Twomey, 1974).

The new sensor is an adaptation of a similar instrument, the PVM-100, used for ground-based measurements of LWC; see Gerber (1991) and Arends et al. (1992). Both instruments utilize light diffracted in the forward direction by cloud droplets to measure integrated droplet properties. The PVM-100A differs primarily from the PVM-100 in that its probe is designed for mounting on the outside of aircraft, its faster electronics cope with aircraft speeds and its two channels simultaneously measure LWC and PSA for the same cloud volume.

The development of the PVM-100A is an attempt to improve the accuracy of measuring LWC and PSA of cloud droplets from aircraft. Present instruments for measuring LWC include the Johnson–Williams (JW) hot-wire probe, the CSIRO hot-wire probe (also called the King probe; King et al., 1978) and the Forward Scattering Spectrometer Probe (FSSP-100; Particle Measuring Systems, Boulder, CO). The JW has a significant dependence on air speed (Strapp and Schemenauer, 1982); the King probe (KP) agrees to within 15% of values calculated using the icing-cylinder calibration technique (King et al., 1985) for droplet sizes within its design range (Biter et al., 1987); and the FSSP-100 gives LWC with the best accuracy by applying corrections for coincidence and deadtime losses, and time-response and laser-inhomogeneity errors (e.g., see Baumgardner et al., 1985; Cooper, 1988; Brenguier, 1989; Brenguier and Amodei, 1989; Baumgardner and Spowart, 1990). Given that existing FSSP-100 differ from each other means that these corrections cannot be entirely adequate unless the variables of each instrument are identified (Cooper, 1988; Baumgardner and Spowart, 1990). In contrast to the preceding three techniques, the PVM-100A does not depend on the rate at which droplets either impact or pass through the instrument; its output is independent of air speed. The PVM instruments look at many droplets simultaneously in a cloud volume about 50,000 larger than the sensitive volume in FSSP-100, where droplets are measured optically individually and summed for LWC. These differences give the PVM the potential of measuring LWC more accurately.

The following decribes the calibration of the PVM-100A in the CHIEF (Chamber for Investigations with Equilibrated Fog; Mallant, 1988) located at Netherlands Energy Research Foundation (ECN), Petten. The PVM-100A is compared to LWC measured with the filter method, as done previously with the PVM-100 (Arends et al., 1992). The calibration of the PSA channel has inherently greater uncertainty, because it relies on comparing in the chamber the PVM-100A with a FSSP-100. Also described are results of measurements with the PVM-100A during ASTEX (Atlantic Stratocumulus Transition Experiment), where the instrument was mounted near other cloud microphysical probes on the University of Washington's C-131A during the 4-week experiment in June 1992. Comparisons are shown between the JW, KP, FSSP-100 and PVM-100A.

INSTRUMENTATION

The probe for the PVM-100A is shown in Fig. 1. It consists of a 11.4-cm-diameter tube which faces into the wind direction during flight. The longer cylindrical housing to the left of the tube contains the laser-diode light source and collimating optics, and mounting holes for attaching the 1.9-kg probe to an aircraft pylon or another mounting arrangement. The shorter housing on the right contains the optics and detectors for the LWC and PSA channels. The laser beam traverses the sampling tube where it irradiates a volume of 1.25 cm^3. The probe is connected by cable to an electronic box located inside the aircraft. The electronics use synchronous detection to separate signals produced in two photodiode detectors by light scattered from the droplets,

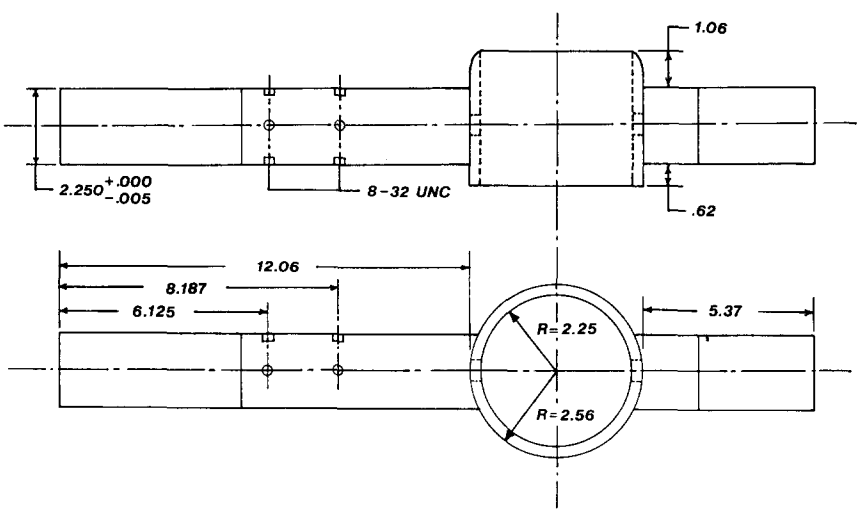

Fig. 1. Probe of PVM-100A; top view (upper) and rear view (lower). Dimensions in inches.

from background light. The electronics also scale the signals, and output analog voltages for LWC, PSA and r_e. The bandpass of the outputs is defined as the 3-db roll-off frequency of symmetrical low-pass filters located in the electronics just prior to the outputs. The roll-off frequency is adjustable and has an upper limit of about 5 KHz, which corresponds to two cycles of illumination of a particle passing through the center of the modulated laser beam at an airspeed of 80 m/s.

The principle of operation of the PVM is illustrated in Fig. 2. Cloud droplets (or other particles such as ice crystals) scatter light into the near-forward direction into a lens that focuses the scattered light onto a variable-transmission filter and sensor for each channel. This arrangement resembles a class of commercial instruments usually called "laser-diffraction particle-sizing instruments"; see Azzopardi (1979) and Hirleman (1984). These instruments utilize a segmented multi-element sensor from which outputs are mathematically inverted to derive droplet spectra. The PVM uses instead variable-transmission filters with transmission function derived by mathematically inverting the integral that describes the flux of scattered light measured by the large area sensors, to directly output LWC or PSA. Similar direct means for measuring such integrated properties of suspended particles have been described previously in the literature (e.g., Stetter, 1949; Breuer, 1960; Wertheimer and Wilcock, 1976; Blyth et al., 1984; Gerber, 1984)

The method used to establish LWC and other desired responses of the PVM is fully described in Gerber (1991), and will only be summarized in the following for the case of LWC:

The equation for LWC is given by

$$\mathrm{LWC}=\frac{4\pi\rho}{3}\int r^3 n(r)\mathrm{d}r \tag{1}$$

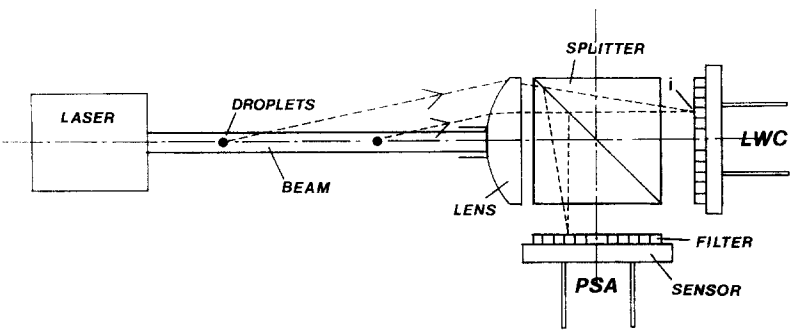

Fig. 2. Sketch of main optical components and operating principle of the PVM-100A. Cubic beamsplitter divides scattered light 50%/50%. Filters with concentric regions of different transmittance weight the scattered light to produce sensor outputs proportional to LWC and PSA.

where r is the droplet radius, $n(r)$ is the droplet size spectrum dn/dr, and $\rho = 1.0\ g/cm^3$ is the droplet density.

If the scattered-light flux measured by the LWC sensor (see Fig. 2) for droplets of radius r is given by $F(r)$, then the equation

$$F(r) = k_1 r^3 \tag{2}$$

must be shown to be valid for the PVM to properly measure LWC; k_1 is a constant.

If the filter consists of annular segments identified by the letter i, then

$$F(r) = \sum_{i=1}^{N} f_i(r) T_i \tag{3}$$

where $f_i(r)$ is the flux of diffracted light incident on i, T_i is the transmission of filter annulus i, and N is the total number of annuli.

The expression for

$$f_i(r) = k_2 l_i r^2 [(J_0^2 + J_1^2)_{i1} - (J_0^2 + J_1^2)_{i2}] \tag{4}$$

is the same as given by Swithenbank et al. (1976), except for the factor l_i which compensates for vignetting effects in the PVM; k_2 is a constant. J_o and J_1 are Bessel functions of the first kind (zeroeth and first order, respectively), and the indices 1 and 2 of the Bessel functions denote boundaries of each annulus ring.

In order to achieve the required relationship shown in Eq. (2), the proper function of T_i must be found in Eq. (3). This is done by mathematically inverting Eq. (3) to determine T_i. Equation (3) is the discrete form of a Fredholm integral of the first kind which is inverted with the condition that Eq. (2) holds. A resulting curve of T_i vs. annulus number is shown in Gerber (1991). The filter with this distribution of T_i gives a predicted bandpass of about 4-μm to 45-μm droplet diameter over which the reponse of the PVM is linear with LWC. Outside of this range the response gradually rolls off with a 50% underestimate of LWC at about 2 μm and 70 μm. A filter with this response is presently used in both the PVM-100A and PVM-100.

CALIBRATIONS AT ECN

(1) CHIEF fog chamber

The CHIEF fog chamber at ECN, Petten, The Netherlands is illustrated in the schematic in Fig. 3. Ambient air enters A, is filtered in B, and passes into the $\sim$4-m^3 chamber C where water trickling over many porous ceramic rings is used to humidify the air to near 100% relative humidity (RH). Atomizers add droplets to the flow at G, which enters the 20-m^3 chamber D where the

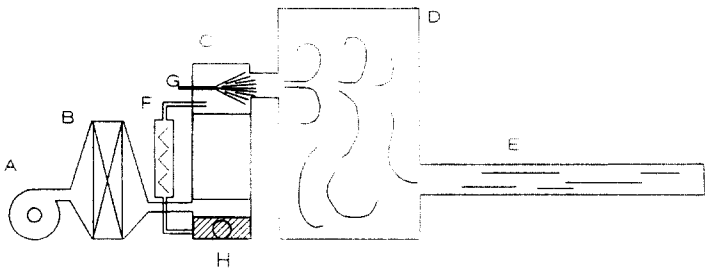

Fig. 3. Schematic of fog-wind tunnel at ECN. *A* (blower), *B* (filter), *C* (humidifying chamber), *D* (mixing chamber), *E* (test section), *F* (heater), *G* (droplet generator), *H* (water pump) (from Mallant, 1988).

air and droplets mix. The flow then passes through a 5-m long test section *E* with a 50-cm by 50-cm cross section. Instruments to measure droplet properties are placed about halfway along *E*. A key feature of the chamber is that the temperature in *E* is used to regulate the water temperature in the humidifier *C* with the heater *F* so that the RH in the chamber remains stable, and so that the fogs generated in the chamber also remain stable for as long as the droplet generators at *G* produce constant outputs.

The fogs are characterized in *E* by measuring the LWC with the filter method, and measuring the droplet spectra with a FSSP-100. Two filter systems are run side by side as a check of the measurement procedure. The filters consist of hydrophobic Pall filters placed in housings that face the flow. Air is drawn through the filters isokinetically at 2.15 m/s and the flow rate filters are conditioned in the operating chamber for at least 2 h before LWC is measured by weighing the filter both before and after a specified time interval, generally on the order of 1 h. The constant high RH in the chamber, and this filter-sampling procedure should minimize LWC measurement errors due to evaporation or growth of droplets collected in the filter. Such errors may be important when the filter method is used under ambient conditions where RH can be subsaturated or supersaturated (e.g., see Valente et al., 1989). The estimated accuracy of filter measurements of LWC in the chamber is 10%.

The FSSP-100 is located near the filters in the test section E. Droplet spectra measured during the present calibration of the PVM-100A are shown in Fig. 4. These spectra are typical of those measured in a previous calibration (Arends et al., 1992), with the exception that spectra were previously limited to droplet volume median diameters (VMD) of 20 μm or smaller. In the present calibration larger VMD were used in order to test the limit of large-particle sensitivity of the instruments. The present calibration also differed from the preceding calibrations in that larger LWC values up to about 1 g/m^3 were generated in the CHIEF. Each spectrum in Fig. 4 is a normalized average of three sets of tests in the chamber, where the sets have similar VMD near

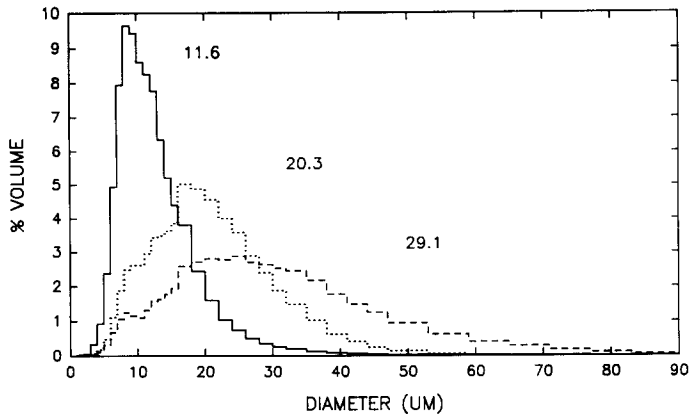

Fig. 4. Droplet size spectra generated in the ECN chamber for calibration of the PVM-100A. Numbers refer to volume median diameters (μm), VMD, of the spectra.

TABLE 1

ECN calibration tests of the PVM-100A. Nebulizer types: H=Heyer 77 ultrasonic; L=Lee Instac pneumatic; W=Wagner 220 ultrasonic. (p) denotes low-pressure operation. FSSP correction is for compensating dead-time and coincidence errors, calculated from Baumgardner et al. (1985)

Test No.	Neb. Type	Filter LWC (g/m^3)	FSSP LWC (g/m^3)	FSSP PSA (cm^2/m^3)	FSSP VMD (μm)	FSSP Conc. ($no./cm^3$)	FSSP Corr.	PVM LWC (V)	PVM PSA (V)
1	1H	0.1376	0.132	800	10.2	452	1.135	0.0452	0.0985
2	2H	0.2038	0.224	1210	11.7	496	1.149	0.0829	0.1710
3	3H	0.2899	0.282	1390	12.9	456	1.137	0.1214	0.2285
4	1L	0.3022	0.407	1520	18.9	427	1.127	0.1184	0.1600
5	2L	0.4952	0.692	2330	20.5	490	1.147	0.2052	0.2685
6	2L(p)	0.2743	0.491	1260	29.4	249	1.072	0.0819	0.0835
7	1L(p)	0.1438	0.281	701	30.1	139	1.040	0.0434	0.0445
8	3L	0.7575	0.940	2930	21.5	471	1.141	0.2880	0.3935
9	1W	0.4809	0.924	1690	40.6	169	1.049	0.0939	0.0860
10	1W,3L	0.9587	1.510	3720	27.8	468	1.140	0.3374	0.4260

10 μm (tests 1, 2, 3), 20 μm (tests 4, 5, 8) and 30 μm (tests 6, 7, 10); see Table 1.

(2) Calibration of PVM-100

The previous calibration of the PVM-100 for LWC is briefly reviewed here, because those results have bearing on the method of analyzing the present calibration of the PVM-100A. The PVM-100 was calibrated by comparing it to infrared extinction measurements made through fogs with various droplet

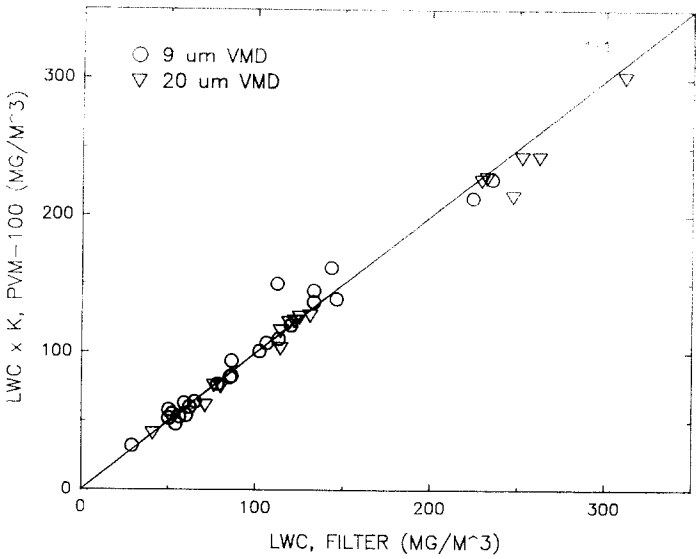

Fig. 5. Comparison of LWC measured with the ground-based instrument, PVM-100, and the filter method in the ECN chamber for two VMD. $K = 1.05$.

spectra in the Calspan Corp., Buffalo environmental chamber (Gerber, 1991). Given that infrared extinction at ~ 11-μm radiation was predicted to be proportional to LWC according to Mie theory (Chýlek, 1978), and verified as such (Pinnick et al., 1979; Gertler and Steele, 1980; Nolan and Jennings, 1987), permitted the scaling constant relating voltage output of the PVM-100 and LWC to be determined.

The PVM-100 was also compared to the filter method as described by Arends (1992). Figure 5 shows this comparison. K, the mean ratio of LWC(Filter)/LWC(PVM-100) for the data in this plot, is equal to 1.05 with sample standard deviation $s = 0.0845$. This difference indicates that the PVM-100, as calibrated against the infrared transmissometer, gives LWC values smaller by 5% on the average than LWC determined with the ECN filters. The value of K depends in part on the relationship between LWC and infrared extinction; the relationship given by Nolan and Jennings (1987) is used here. The correlation coefficient between data sets in Fig. 5 is 0.991, and K differs by less than 5% for the two values of VMD. This good agreement of LWC measured independently by two fundamental calibration techniques suggests that LWC is being measured accurately by the PVM-100 over the given VMD range.

(3) Calibration of PVM-100A

The procedure for calibrating the new aircraft probe, PVM-100A, consists

of first producing a reference voltage output for each channel that can be easily reproduced. This is done by placing a light diffusing disk against the receiver-tube aperture, and adjusting the instrument's gain to choose a reference voltage. The reference voltages chosen for the PVM-100A were 0.075 V for the LWC channel and 0.500 V for the PSA channel. The next step is to compare the output of each channel to a standard method of measuring LWC and PSA to determine scaling constants K_1 and K_2 required to scale the PVM-100A voltages:

$$\text{LWC(Standard; g/m}^3\text{)} = \text{PVM(Volts)} \times K_1 \text{ (g/m}^3\text{/Volts)} \quad (5)$$

$$\text{PSA(Standard; cm}^2\text{/m}^3\text{)} = \text{PVM(Volts)} \times K_2 \text{ (cm}^2\text{/m}^3\text{/Volts)} \quad (6)$$

The ECN filter method is used as the standard for LWC. The values of LWC measured by the filters, Table 1, are averages of the two adjacent filters used simultaneously for each test. The mean difference between filters is 2.86%. K_1 is determined by averaging K_1 values calculated for some of the tests listed in Table 1. Given the previous good agreement between LWC measured by the PVM-100 and the ECN filter method for VMD $\sim$ 20 μm and smaller, this averaging is limited to the tests in Table 1 where VMD is $\sim$10 μm (tests 1, 2, 3) and $\sim$20 μm (tests 4, 5, 8). The value of K_1 determined in this fashion is 2.58 with s=0.241. Figure 6 shows the relationship between LWC measured by the filter and PVM-100A after this scaling con-

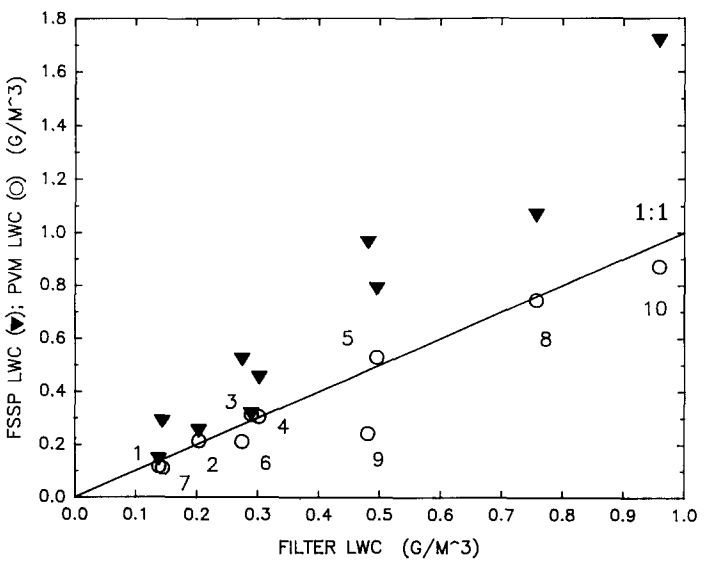

Fig. 6. Comparisons of LWC measured with the FSSP-100, the filter method, and the PVM-100A in the ECN chamber during the calibration of the PVM-100A. A scaling factor of 2.58 is applied to the PVM-100A output voltage to calculate LWC. Numbers indicate test numbers given in Table 1.

stant is applied to all the PVM-100A measurements. The PVM-100A LWC with VMD $\sim 10\,\mu$m and $\sim 20\,\mu$m shows a highly linear relationship with filter LWC as also noted in the previous calibration. Tests 6, 7 and 10 for which VMD $\sim 30\,\mu$m shows that the PVM-100A underestimates the filter LWC by a mean value of 18%. This value is reasonably close to the expected underestimate of $\sim 15\%$, predicted by applying the particle-size bandpass of the LWC filter used in the instrument to the measured droplet spectrum (Fig. 4). Test 9 shows an underestimate in the PVM-100A LWC of $\sim 50\%$. For this test, the Wagner nebulizer produced some droplets that were beyond the size limit of the largest FSSP-100 size bin (89 μm–95 μm). Thus the measured VMD of 40.6 μm for this test is an underestimate of the true unknown value of VMD.

The FSSP-100 is used as the standard for determining the scaling constant K_2 for PSA. This requires that the FSSP-100 produces accurate values of PSA. We see from Fig. 6 that the FSSP-100 significantly overestimates LWC for most of the tests, so that values of PSA calculated from the FSSP-100 droplet spectra will be inaccurate and will also show overestimates. This trend in LWC measured by the FSSP-100 was noted previously by Arends et al. (1992) during the calibration where FSSP-100 and PVM-100 were compared; one of us (B.G.A.) is presently investigating this result. The magnitude of the overestimate in LWC, given by the ratio of the LWC measured by the FSSP-100 and the filter, increases as a function of VMD; see Fig. 7. The tests show a linear increase in this ratio with VMD, except for test 9, which is not included in the subsequent analyses.

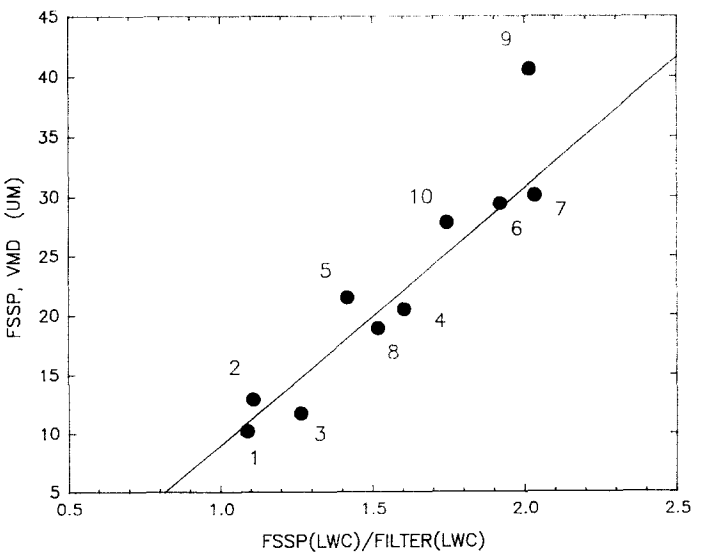

Fig. 7. VMD of droplet spectra measured by the FSSP-100 vs. the ratio of FSSP LWC to filter LWC.

The value of K_2 is estimated by comparing the voltage output of the PVM-100A PSA channel to values of PSA measured with the FSSP-100 and corrected for the overestimates. Given that this FSSP-100 was exposed to monodisperse glass beads, which showed proper sizing by the instrument, suggests that the error is related to concentration overestimates.

The determination of the PSA correction consists of an inversion problem as shown by the following integral for LWC, which should be compared with Eq. (1):

$$\text{FILTER(LWC)} = \frac{4\pi}{3} \int c(r,n) r'^3 n'(r') \mathrm{d}r' \tag{7}$$

where the volume size spectrum measured by the FSSP-100 is given by $r'^3 n'(r')$, $n'(r') = \mathrm{d}n'/\mathrm{d}r'$, $c(r,n)$ is the correction function, and FILTER(LWC) is assumed to be the correct measure of LWC. It is necessary to solve for $c(r,n)$ which can then be used to find the correction for the PSA integrals of the FSSP-100 data.

If we assume that $\mathrm{d}n'$ has been measured correctly, that is $n'(r') = n(r')$, and that the overestimate is in r' (contrary to the glass-bead evidence), then $c(r,n) = r^3/r'^3$. If we further assume that r' and r are related by $r = r'$x [FILTER(LWC)/FSSP(LWC)]$^{1/3}$, then $c(r,n)$ is given by the reciprocal, FILTER(LWC)/FSSP(LWC), of FSSP-100 LWC error. This gives [FILTER(LWC)/FSSP(LWC)]$^{2/3}$ as the correction for the surface integrals. The corrected PSA values are shown in Fig. 8 (dots). The mean value of K_2 determined with Eq. (6) from the corrected values of PSA is 7700 with $s = 749$.

If we now assume that the FSSP-100 accurately measures r', and instead overestimates $\mathrm{d}n'$, that is $n'(r') = n'(r)$, then $c(r,n) = n(r)/n'(r) = g(r)$, where $g(r)$ is an unknown function of r. Given that an integral similar to Eq. (7) exists for each of the 9 tests, which must each include the same $g(r)$, it is possible to estimate the dependence of $g(r)$ on r. Figure 9 shows a second-order polynomial fitted to 8 data points consisting of Y = FSSP VMD and the ratio X = FILTER(LWC)/FSSP(LWC). The non-experimental data point at $Y = 100$ μm, $X = 0$ is added to subjectively extrapolate the curve to the left of the seven experimental data points, and to provide values of X and Y for $Y > 30$ μm; and X is assigned a value of 1.0 for $Y < 12$ μm to extrapolate the curve (not shown in Fig. 9) to the right of the experimental data. The correction function g(r) is given by the polynomial in Fig. 9 solved for X (for $Y > 12$ μm), that is $X = f(Y) = g(r)$, which applies to both the LWC and PSA integrals of the FSSP-100. A test of the fit of $g(r)$ is to apply $g(r)$ to each size bin of the FSSP-100 LWC spectra for all the tests, and to see if the correct filter LWC results. The mean difference between the corrected LWC and the filter LWC is within 1% with a correlation coefficient of 0.995. When $g(r)$ is applied to the FSSP-100 PSA integrals, corrected PSA values result (Fig. 8, cir-

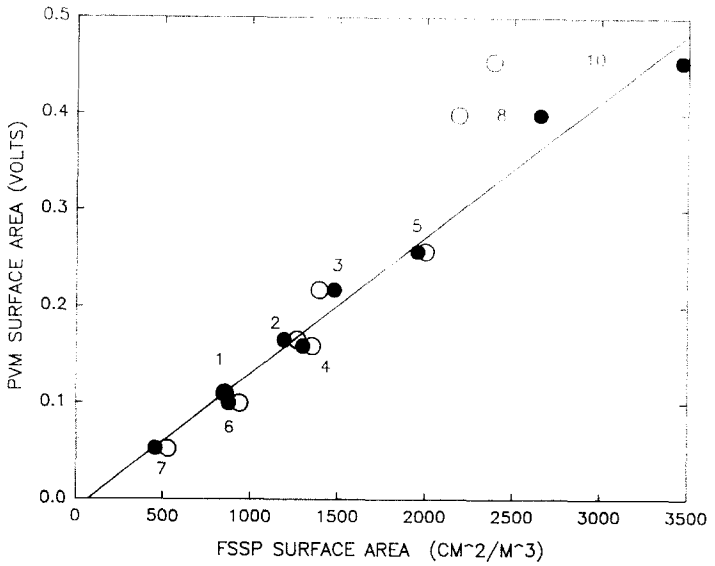

Fig. 8. Comparison of the PVM-100A voltage output for droplet surface area (PSA) and PSA calculated from the FSSP-100 spectra. See text for the significance of the dot and circle data.

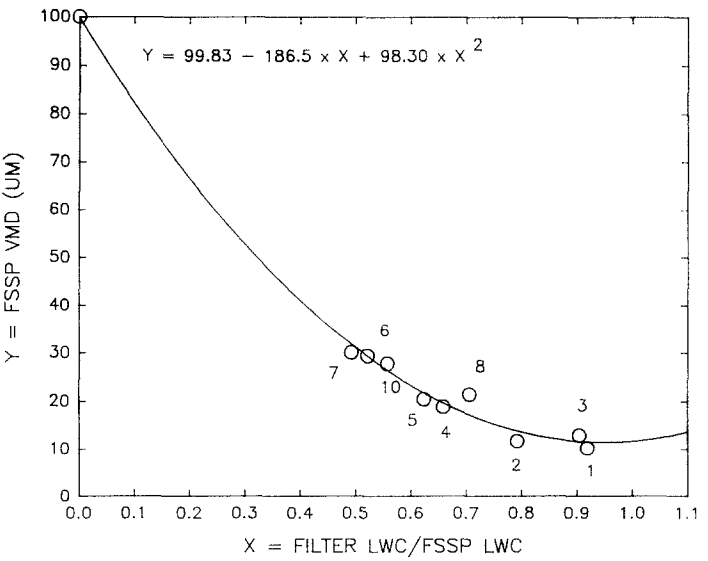

Fig. 9. VMD measured by the FSSP-100 (except upper left point) as a function of the ratio of FSSP LWC to filter LWC. Curve is given by second-order polynomial shown fitted to data.

cles) from which a mean value of $K_2 = 7584$ $s = 1634$ is found. The close agreement of K_2 found for the preceding two methods indicates that the PSA correction is independent of whether r or n causes the overestimates. Given

that FILTER(LWC) is proportional to the product r'^3n' in Eq. (7), suggests that the two preceding correction schemes are equivalent mathematically. In subsequent calculations $K_2=7700$ is used, because of the corresponding smaller value of s.

In the preceding estimates of K_2 we have used FSSP-100 data corrected for coincidence and dead-time errors (see Table 1) according to the formulation of Baumgardner et al. (1985). The influence of these corrections on the value of K_2 is small; however, the effectiveness of the corrections is evident, since they significantly reduce the corresponding value of s. Given the relatively slow air speed of 27.4 m/s through the FSSP-100 during the tests, the correction for time-response error given by Baumgardner and Spowart (1990) was not applied.

An independent validation of the preceding PSA calibration is recommended. Exposing the PVM-100A to monodisperse glass beads in a vertical sedimentation tunnel is suggested as an appropriate approach for such a calibration, because the output of the instrument is independent of the speed of the particles.

AIRCRAFT MEASUREMENTS

The PVM-100A was flown on the University of Washington's C-131A during the ASTEX Project in June 1992. It was mounted on the lower half of the fuselage about 3-m behind the nose of the aircraft, and in close proximity to a JW hot-wire probe, a King hot-wire probe and another FSSP-100. The C-131A flew 16 missions during ASTEX, with a total of about 75 h flight time. Conditions experienced during the flights included heavy drizzle and rainfall, droplet concentrations from about 30/cm^3 to 800/cm^3 (uncorrected FSSP-100 data), and clouds with LWC near 3 g/m^3. The PVM-100A operated in a stable fashion during the flights, with minimal changes in optics and electronics. The following is not intended to provide an in-depth comparison of the preceding probes, but will be limited to presenting a few examples of the collected data.

Figure 10 compares LWC measured by the JW, King probe, FSSP-100 and PVM-100A during a short segment of a flight passing through broken stratocumuli. The sampling rate of the data recording system aboard the C-131A was 10 Hz. The JW produced the smallest values of LWC. Both commercial hot-wire probes showed hysteresis in their response time, so that inter-cloud gaps were not resolved in comparison to the output of the faster-responding PVM-100A.

Figure 11 compares LWC measured by the King probe, FSSP-100 and PVM-100A during an ascent through a stratocumulus layer that was noteworthy for showing a small amount of entrainment at its upper surface. This layer differed from nearly all others in that local regions of lowered LWC, which are

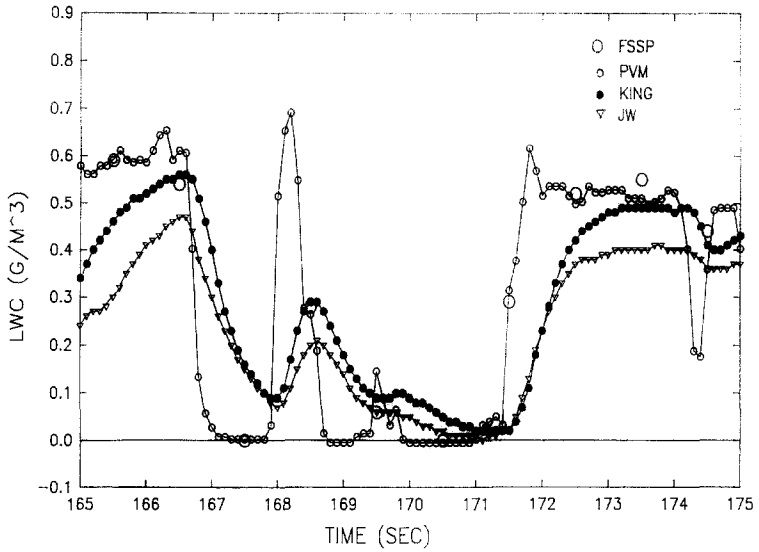

Fig. 10. Comparison of LWC measured by the FSSP-100, PVM-100A, JW and King probes in a broken cloud field traversed by the Univ. of Washington C-131A aircraft during ASTEX.

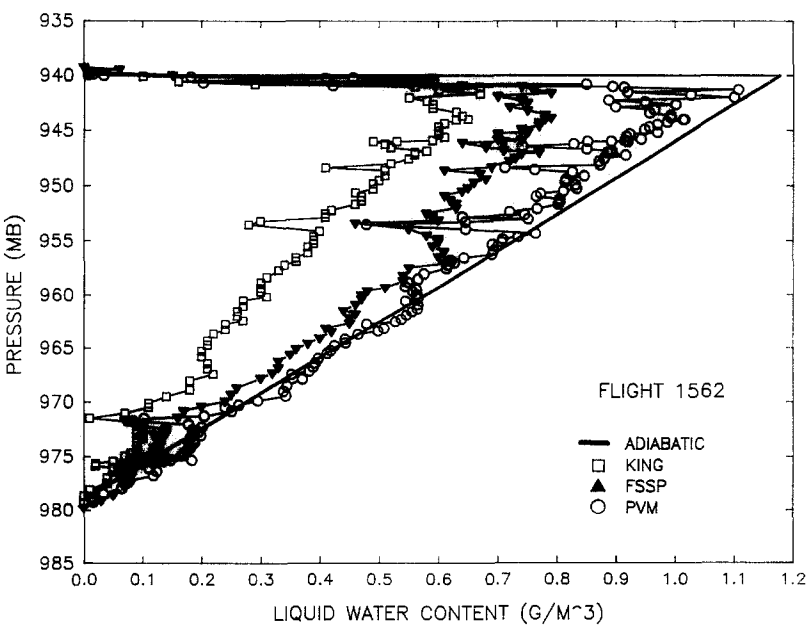

Fig. 11. Comparison of LWC measured by the FSSP-100, PVM-100A and King probes during a vertical traverse of a marine stratocumulus layer by the C-131A with the calculated adiabatic LWC profile.

indicative of the entrainment into cloud top of drier air, were minimal. Also, the droplet concentration in this layer was unusually stable. The lack of significant entrainment in this layer may have been due to the known existence of a higher cloud layer shielding this layer from radiative effects that influence entrainment. This layer should show a LWC profile that is nearly adiabatic, because of the low entrainment. The King probe significantly underestimates the adiabatic LWC profile; this probe usually gave better results, but was erratic on occasion. The FSSP-100 data, to which no corrections were applied, shows a typical rolloff in LWC seen when either LWC increases to larger values or the droplet spectrum shifts to larger droplet sizes. These trends are symptomatic of the aircraft use of the FSSP-100, and are opposite to the trend found for the low-speed use of the ECN FSSP-100 described in the wind tunnel calibration. The PVM-100A shows the best agreement with the adiabatic LWC profile in Fig. 11. This is indirect evidence that the LWC calibration was done correctly, under the assumptions that cloud-top entrainment and the effect of drizzle were minimal, and that the cloud layer was horizontally homogeneous over the distance required for the aircraft to complete the profile.

Figure 12 compares r_e ($K_1=2.58$, $K_2=7700$) measured by the PVM-100

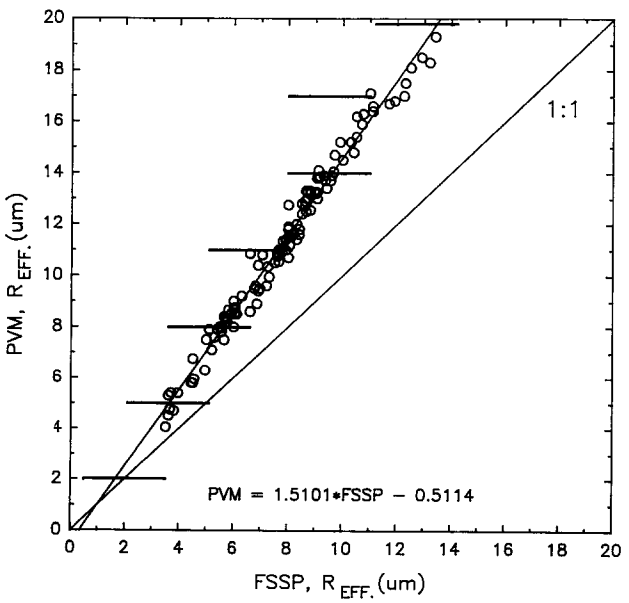

Fig. 12. Effective droplet radius measured by co-located FSSP- 100 and PVM-100A on the C-131A (circles). Horizontal bars show the results of calculations comparing droplet diameters (horizontal axis) measured with a FSSP-100 at an airspeed of 80 m/s to the true droplet diameters (vertical axis); from Baumgardner and Spowart (1990). Linear regression gives the straight line through the PVM-100A data.

and the University of Washington FSSP-100 (uncorrected) in marine boundary layer clouds during ASTEX. The data represent 1-min averages of r_e taken from 500 km of in-cloud flight distance (average aircraft speed was 83 m/s), and represent a wide range in droplet size distributions; cases with drizzle are not included, because for those cases some droplet sizes fall outside the measurement ranges of both instruments. The difference in Fig. 12 between r_e measured by FSSP-100 and PVM-100A is highly correlated, and shows a regression relationship where the measurements differ by approximately a constant factor that is linear with effective radius. This result is similar in magnitude and direction to the calculated "time-response and laser-inhomogeneity" errors of the FSSP-100 for an airspeed of 80 m/s (Baumgardner and Spowart, 1990). These errors, shown in Fig. 5 of the paper of Baumgardner and Spowart (1990), are reproduced as the horizontal bars in Fig. 12, and are, according to these authors, a result of the FSSP-100 underestimating droplet sizes by approximately a constant factor. For a given FSSP-100 and airspeed, this constant factor should appear unchanged in the measurement of r_e and be independent of droplet concentration, because of the definition of r_e. The intercomparisons in Fig. 12 indicate that the differences in r_e measured by the PVM-100A and FSSP-100 during ASTEX may be a result of the time-response and laser-inhomogeneity errors of the FSSP-100.

This result suggests that flying both the FSSP-100 and PVM-100 together on the same research aircraft may significantly improve the accuracy of the droplet spectra measured by FSSP-100 by correcting them with PVM-100A measurements. The suggested procedure would partition time-response and laser-inhomogeneity errors from concentration errors in the following sequence:

(1) The ratio between r_e, established by comparing PVM-100A and FSSP-100 r_e measurements, is used to correct the shape of the FSSP-100 droplet size spectrum.

(2) The LWC measured by the PVM-100 is used to scale the FSSP-100 LWC, thus correcting the FSSP-100 concentration errors.

(3) A correction is applied to the droplet spectrum to eliminate the small number of "large droplets" caused by the coincidence of smaller droplets in the FSSP-100 sample volume (Cooper, 1988).

The accuracy of this procedure depends on the accuracy of the PVM-100A calibration and the results of Baumgardner and Spowart (1990). At the least, the high expected precision of the PVM-100A, such as has been found for the PVM-100, would permit various FSSP-100 flown with the PVM-100A to be compared with each other better than before.

ACKNOWLEDGMENTS

Gabor Vali of the University of Wyoming is thanked for his contribution to the design of the new aircraft probe. We thank Gerard Kos of ECN for his

fine effort during the ECN calibration. The help of Jack Russel, Dean Hegg and Ronald Ferek ohf the University of Washington, and of Ken McMillan and Rodney Sorrenson, the pilots of the C-131A, is much appreciated. This work was supported by NSF Grants ATM-9207345 and ATM-9204149, NASA Grants NAG2-777 and NCA2-623, and NASA P.O. 913-44468.

REFERENCES

Arends, B.B., Kos, G.P.A., Wobrock, W., Schell, D., Noone, K.J., Fuzzi, S. and Pahl, S., 1992. Comparison of techniques for measurements of fog liquid water content. Tellus, 44B: 604–611.

Azzopardi, B.J., 1979. Measurement of drop sizes. Int. J. Heat Mass Transfer, 22: 1245–1279.

Baumgardner, D. and Spowart, M., 1990. Evaluation of forward scattering spectrometer probe. Part III: Time response and laser inhomogeneity limitations. J. Atmos. Oceanic Technol., 7: 666–672.

Baumgardner, D., Strapp, W. and Dye, J.E., 1985. Evaluation of the forward scattering spectrometer probe. Part II: Corrections for coincidence and dead-time losses. J. Atmos. Oceanic Technol., 2: 626–632.

Biter, C.J., Dye, J.E., Huffman, D. and King, W.D., 1987. The drop-size response of the CSIRO liquid water probe. J. Atmos. Oceanic Technol., 4: 359–367.

Blyth, A.M., Chittenden, A.M.I. and Latham, J. 1984. An optical device for the measurement of liquid water content in clouds. Q. J. R. Meteorol. Soc., 110: 53–63.

Brenguier, J.L., 1989. Coincidence and dead-time corrections for particle counters. Part II: High concentration measurements with an FSSP. J. Atmos. Oceanic Technol., 6: 585–598.

Brenguier, J.L. and Amodei, L., 1989. Coincidence and dead-time corrections for particle counters. Part I: A general mathematical formalism. J. Atmos. Oceanic Technol., 6: 575–584.

Breuer, H., 1960. Staubmessungen im Steinkohlenbergbau. Staub, 20: 290–296.

Chýlek, P., 1978. Extinction and liquid water content of fogs and clouds. J. Atmos. Sci., 35: 296–300.

Cooper, W.A., 1988. Effects of coincidence on measurements with a forward scattering spectrometer probe. J. Atmos. Oceanic Technol., 5: 823–832.

Gerber, H., 1984. Liquid water content of fogs and hazes from visible light scattering. J. Climate Appl. Meteorol., 23: 1247–1252.

Gerber, H., 1991. Direct measurement of suspended particulate volume concentration and far-infrared extinction coefficient with a laser-diffraction instrument. Appl. Opt., 30: 4824–4831.

Gerber, H., 1992. New microphysics sensor for aircraft use. Proc. 11th Int. Conf. Clouds and Precipitation, Montreal, 1992, pp. 942–944.

Gertler, A.W. and Steele, R.L., 1980. Experimental verification of the linear relationship between ir extinction and liquid water content of clouds. J. Appl. Meteorol., 19: 1314–1317.

Hansen, J.E. and Travis, L.D., 1974. Light scattering in planetary atmospheres. Space Sci. Rev., 16: 527–610.

Hirleman, E.D., 1984. Particle sizing by optical nonimaging techniques. In: J.M. Tishkoff (Editor), Liquid Particle Size Measurement Techniques. Am. Soc. Test Mater. Spec. Tech. Publ., 848: 39–48.

King, W.D., Dye, J.E., Strapp, J.W., Baumgardner, D. and Huffman, D., 1985. Icing wind tunnel tests on the CSIRO liquid water probe. J. Atmos. Oceanic Technol., 2: 340–352.

King, W.D., Parkin, D.A. and Handsworth, R.J., 1978. Hot-wire water device having fully calculable response characteristics. J. Appl. Meteorol., 17: 1809–1813.

Mallant, R.K.A.M., 1988. A fog chamber and wind tunnel facility for calibration of cloud water collectors. In: M.H. Unworth and D. Fowler (Editors), Acid Deposition at High Elevation Sites. Kluwer, Dordrecht, pp. 479–490.

Nolan, P.F. and Jennings, S.G., 1987. Extinction and liquid water content measurements at CO_2 laser wavelengths. J. Atmos. Oceanic Technol., 4: 491–400.

Pinnick, R.G., Jennings, S.G., Chylek, P. and Auverman, H.V., 1979. Verification of a linear relationship between IR extinction, absorption and liquid water content of fogs. J. Atmos. Sci., 36: 1577–1586.

Stetter, G., 1949. Dust inspection by optical measurements. Microtecnic, 3: 234–239.

Strapp, J.W. and Schemenauer, 1982. Calibration of Johnson– Williams liquid water content meters in a high-speed icing tunnel. J. Appl. Meteorol., 21: 98–108.

Swithenbank, J., Beer, J.M., Taylor, D.E.S., Abbot, D. and McCreath, G.C., 1976. A laser diagnostic for the measurement of droplet and particle size distributions. Prog. Astronaut. Aeronaut., 53: 421–429.

Twomey, S., 1974. Pollution and the planetary albedo. Atmos. Environ., 8, 1251–1256.

Valente, R.J., Mallant, R.K.A.M., McLaren, S.E., Schemenauer, R.S. and Stogner, R.E., 1989. Field intercomparison of ground-based cloud physics instruments at Whitetop Mountain, Virginia. J. Atmos. Oceanic Technol., 6: 396–406.

Wertheimer, A.L. and Wilcock, W.L., 1976. Light scattering measurements of particle distributions. Appl. Opt., 15: 1616–1620.